International Journal of Environmental Sciences
ISSN: 2229-7359
Vol. 6 No. 1, 2020
https://www.theaspd.com/ijes.php

Selective Photodegradation of Alizarin Using Molecularly Imprinted Cu-Doped TiO_2 Photocatalysts

Simrat Kaur[a], Seema Maheshwari*[a]
[a] Department of Chemistry, Mata Gujri College, Fatehgarh Sahib-140406, Punjab, India
*Corresponding Author's email id: maheshwaris@gmail.com

Received: 04.01.2020 *Accepted: 07.02.2020* *Published: 27.02.2020*
DOI: https://doi.org/10.64252/dbvsz327

Abstract
The selective removal of dye contaminants from industrial wastewater remains a major challenge in environmental remediation. In this work, molecularly imprinted Cu-doped TiO_2 photocatalysts were synthesized via a sol–gel method using alizarin as a template molecule. The prepared photocatalysts were characterized by Fourier transform infrared spectroscopy (FTIR), X-ray diffraction (XRD), and UV–Vis diffuse reflectance spectroscopy (DRS). XRD analysis confirmed the formation of crystalline anatase TiO_2 with an average crystallite size of approximately 30–35 nm. FTIR spectra revealed characteristic Ti–O–Ti vibrations, indicating the formation of the oxide framework. DRS analysis demonstrated a red shift in the absorption edge after Cu doping, resulting in a reduction of band gap energy from 3.2 eV for pristine TiO_2 to 2.9, 2.7 and 2.5 eV for 0.1%, 0.5% and 1% Cu-doped TiO_2, respectively. Photocatalytic degradation experiments under visible light irradiation revealed that Cu-doped MIP-TiO_2 achieved 83.4% degradation of alizarin within 30 min. The degradation followed pseudo-first-order kinetics with an apparent rate constant of 0.061 min^{-1}, which was significantly higher than that of undoped TiO_2 (0.023 min^{-1}). The improved photocatalytic performance is attributed to the synergistic effects of Cu doping and molecular imprinting, which enhance selective adsorption of the target dye. These results demonstrate that molecularly imprinted Cu-doped TiO_2 photocatalysts are promising materials for selective dye degradation in wastewater treatment.
Keywords: *Alizarin, Molecular imprinting, Cu-doped TiO_2, Photocatalysis, Dye degradation, Visible light.*

1. INTRODUCTION

The discharge of synthetic dyes from textile, leather, pharmaceutical, and printing industries has become a serious environmental concern due to their persistence, toxicity, and resistance to biodegradation [1]. Many dyes possess complex aromatic structures and stable chromophoric groups, which make them highly resistant to conventional biological wastewater treatment processes. When released into aquatic systems, dye pollutants can reduce light penetration, inhibit photosynthetic activity in aquatic organisms, and generate toxic degradation products that pose risks to human health and the environment. Among various dyes, alizarin (1,2-dihydroxyanthraquinone) is widely used in textile dyeing, analytical chemistry, and biological staining. Due to its stable anthraquinone structure and strong chromophoric system, alizarin exhibits high chemical stability and persistence in aquatic environments [2] [3]. Consequently, the development of effective technologies for the removal of alizarin from wastewater is of considerable importance.

Advanced oxidation processes (AOPs) have attracted significant attention for the degradation of persistent organic pollutants. Semiconductor photocatalysis has emerged as a particularly promising approach because it can mineralize organic contaminants into environmentally benign products such as carbon dioxide and water under light irradiation. Titanium dioxide (TiO_2) is one of the most extensively studied photocatalysts owing to its chemical stability, non-toxicity, low cost, and strong oxidative potential [4], [5]. Despite these advantages, TiO_2 photocatalysts exhibit certain limitations. One major drawback is their wide band gap (~3.2 eV for anatase TiO_2), which restricts photoactivity to ultraviolet radiation [6]. Since ultraviolet light represents only a small fraction of the solar spectrum, the photocatalytic efficiency of TiO_2 under natural sunlight remains limited. Additionally, TiO_2 photocatalysts generally lack selectivity toward specific pollutants and may degrade organic molecules indiscriminately in complex wastewater systems. To overcome these limitations, various strategies have been developed to enhance the photocatalytic performance of TiO_2. These include metal doping, semiconductor coupling, surface modification and sensitization with conductive polymers [7], [8], [9]. Metal doping has proven particularly effective for improving photocatalytic efficiency by introducing impurity energy levels within the band structure of TiO_2, thereby extending light absorption into the visible region [10]. Another promising

approach to improve photocatalytic selectivity is molecular imprinting technology (MIT). Molecular imprinting involves polymerization of functional monomers around a template molecule to create recognition cavities within a polymer matrix. After removal of the template molecule, these cavities remain complementary in size, shape and functional groups to the target molecule [11]. Such materials exhibit high selectivity and affinity toward the template molecule. Molecularly imprinted polymers possess several attractive properties including high stability, strong mechanical strength and excellent molecular recognition capability [12]. Because of these features, they have been widely applied in separation science, chemical sensing, catalysis and drug delivery systems [13], [14], [15]. Due to their ability to mimic the recognition properties of biological antibodies, molecularly imprinted polymers are often referred to as plastic antibodies [16]. Traditional imprinting techniques such as bulk polymerization often produce irregular particles with deeply embedded binding sites, which may limit mass transfer and reduce binding efficiency [17]. Surface imprinting techniques have therefore been developed to place recognition sites near the surface of materials, allowing faster binding kinetics and improved accessibility [12]. Combining molecular imprinting with semiconductor photocatalysts has led to the development of molecularly imprinted photocatalysts, which integrate selective adsorption with photocatalytic degradation. In such systems, target molecules are preferentially adsorbed at imprinted recognition sites located near photocatalytic active centers, thereby enhancing degradation efficiency. Several researchers have reported molecularly imprinted TiO_2 photocatalysts for selective degradation of organic pollutants. Sharabi and Paz demonstrated preferential photodegradation of contaminants using molecular imprinting on TiO_2 surfaces [18] . Luo et al. synthesized molecularly imprinted TiO_2/WO_3 nanocomposites capable of selective photocatalytic degradation of target pollutants [19]. Liu et al. reported enhanced photocatalytic activity of molecularly imprinted Co-doped TiO_2 nanocomposites under visible light irradiation [20]. However, further research is required to develop photocatalysts capable of selective recognition and efficient degradation of specific dye molecules such as alizarin.

In the present work, molecularly imprinted Cu-doped TiO_2 photocatalysts were synthesized using the sol–gel method with alizarin as the template molecule. Copper doping was introduced to enhance visible-light absorption and improve photocatalytic performance. The synthesized materials were characterized using various analytical techniques and their adsorption properties, selectivity and photocatalytic activity toward alizarin degradation were systematically investigated.

2. Experimental

2.1 Materials

All chemicals employed in this study were of analytical grade and were used without any further purification. Tetrabutyl orthotitanate (TBOT) (≥97%), Copper nitrate ($Cu(NO_3)_2$), Alizarin, polyethylene glycol (PEG-200) [$H(OCH_2CH_2)_nOH$], Ethanol (absolute, >99.8%) and acetic acid (≥99%) were obtained from Sigma-Aldrich.

2.2 Instrumentation

The prepared materials were characterized using several analytical techniques, including Fourier transform infrared (FT-IR) spectroscopy, diffuse reflectance spectroscopy (DRS), and X-ray diffraction (XRD). The FT-IR spectra were recorded on a Bruker FT-IR spectrometer in the wavenumber range of 400–4000 cm^{-1} using the KBr pellet method for sample preparation. Diffuse reflectance spectra were obtained using a UV–Visible spectrophotometer equipped with an integrating sphere attachment, and the measurements were carried out in the wavelength range of 200–800 nm with $BaSO_4$ employed as the reflectance standard. Prior to optical analysis, the nanoparticle suspensions were sonicated in an ultrasonic bath (Sarthak Scientific Services, India) to achieve uniform dispersion of particles. All measurements were performed under ambient laboratory conditions.

2.3 Synthesis of Molecularly Imprinted Cu-Doped TiO_2 (MIP-Cu-TiO_2)

Molecularly imprinted Cu-doped TiO_2 photocatalysts were synthesized via the sol–gel method as shown in Figure 1. Tetrabutyl orthotitanate (TBOT) (5 mL) was mixed with acetic acid (1mL) and ethanol (15 mL) in 5:1:15 ratio and stirred for 30 min at room temperature. Copper nitrate sol of concentrations 0.1 mol%, 0.5 mol% and 1 mol% relative to Ti was prepared in 10 mL of ethanol and mixed with above solution at 60°C on magnetic stirrer drop by drop. 0.240 g alizarin was added to the mixture and continuously stirred at 60°C until alizarin completely dissolved, then 0.1 mL of 1% Polyethyleneglycol (PEG-200) solution (prepared in ethanol) was added dropwise. The reaction mixture was then allowed to

stir for at least 6 h at 60°C. A gel-like material was obtained which was then allowed to dry in oven at 100°C. Dried sample was then calcined at 400°C in muffle furnace for 2 h. The obtained particles of molecularly imprinted Cu doped TiO_2 and is denoted as MIP/Cu-TiO_2. Similarly non-imprinted Cu doped TiO_2 particles were prepared without adding alizarin dye and is denoted as NIP/Cu-TiO_2.

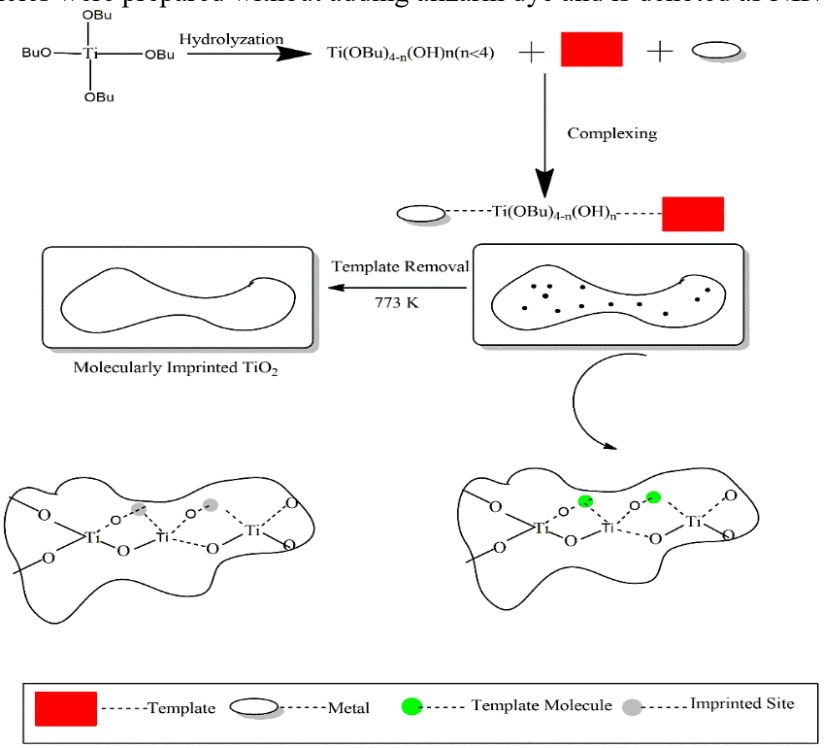

Figure 1: Synthesis of Molecularly Imprinted Cu-Doped TiO_2 Photocatalyst

3. RESULTS AND DISCUSSION

3.1 Rebinding Studies

This study used UV-Vis spectrophotometry to examine the selectivity and binding capacity of alizarin-imprinted titania nanoparticles after complete template removal. Calcination removes alizarin from the doped titania matrix, leaving behind "imprint" cavities. The rebinding of alizarin molecules to these cavities was investigated by immersing 0.02 g of doped imprinted titania photocatalyst in 20 ml of alizarin solutions of varying concentrations (0.01 to 0.095 mmol/L) for 1 hour. The mixture was then centrifuged and the supernatant analysed using a UV/vis spectrophotometer. The amount of alizarin rebound in the titania particles was determined by measuring the difference in absorbance of the alizarin solutions before and after immersion. This data can be used to generate an adsorption isotherm, allowing for quantification of re-included alizarin as shown in Figure 2.

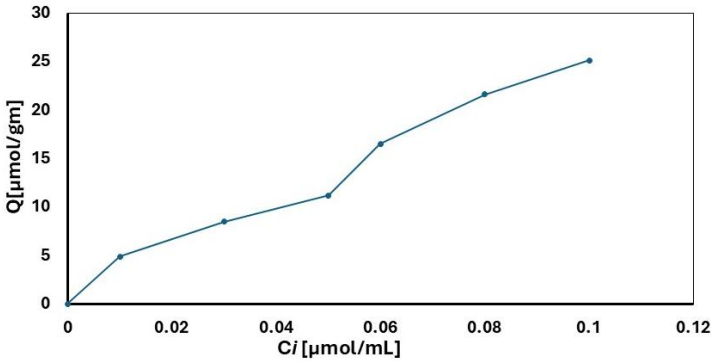

Figure 2: Representation of Adsorption Isotherm for Alizarin

To calculate the adsorption capacity of the titania particles, the exact concentrations of alizarin solutions before and after re-inclusion were measured. This allowed for the calculation of the amount of alizarin adsorbed using the following equation:

$$Q = \frac{(C_i - C_f)V}{m}$$

where: Q is the adsorption capacity (μmol g^{-1}), C_i is the initial concentration of alizarin solution (μmol mL^{-1}), C_f is the final concentration of alizarin solution (μmol mL^{-1}), V is the volume of the solution (mL), m is the mass of imprinted particles (g). By plotting a graph of Ci versus Q, we can analyse the binding affinity of the titania particles for increasing concentrations of alizarin. This graph clearly shows that the recognition ability increases linearly with the concentration of alizarin.

3.2. Characterization techniques:

The structural and optical characteristics of the synthesized materials were investigated using several analytical techniques. Fourier transform infrared (FTIR) spectroscopy was employed to identify the functional groups and bonding interactions present in the samples. X-ray diffraction (XRD) analysis was carried out to determine the crystalline phase, structural purity, and crystallite nature of the prepared materials. In addition, diffuse reflectance spectroscopy (DRS) was used to evaluate the optical absorption behaviour and estimate the band gap properties of the samples. These complementary characterization techniques provide comprehensive information about the structural framework and optical properties of the synthesized materials.

3.2.1 IR Spectra

Figure 3 shows the IR spectra of Cu doped TiO_2 of various samples with different Cu loading samples which were synthesized via sol-gel method in the range of 400–4000cm^{-1}. The distinct band absorption at 1000-400 cm^{-1} is due to Ti–O–Ti stretching vibration, which indicates the formation of TiO_2 [20]. The FTIR spectra of Cu-doped TiO_2 samples show characteristic absorption bands at approximately 795, 780, and 513 cm^{-1}, corresponding to Ti–O and Ti–O–Ti lattice vibrations. The presence of these bands confirms the formation of the TiO_2 framework. No additional peaks related to copper oxide species were observed, suggesting that Cu ions are either incorporated into the TiO_2 lattice or highly dispersed on the surface. The similarity of spectra for different Cu loadings indicates that Cu doping does not significantly alter the TiO_2 crystal structure.

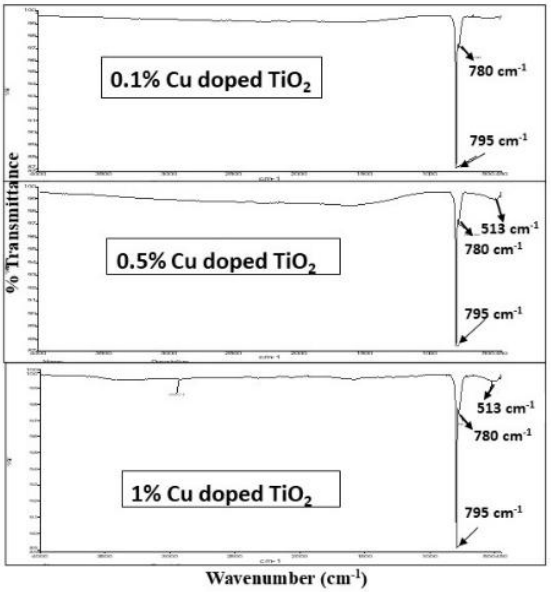

Figure 3: FT-IR spectra of Cu-doped TiO_2 (0.1 mol%, 0.5 mol% and 1 mol% Copper doped TiO_2)

3.2.2 XRD Analysis

The XRD pattern of the synthesized Cu-doped TiO_2 photocatalyst is presented in Figure 4. The absence of separate copper oxide peaks suggests that Cu ions are successfully incorporated into the TiO_2 lattice rather than forming segregated oxide phases. The crystallite size of the photocatalyst was estimated using the Debye–Scherrer equation. The calculated average crystallite size was found to be approximately 30–35 nm, indicating the formation of nanocrystalline TiO_2 particles. No additional diffraction peaks corresponding to CuO or Cu_2O phases were observed, indicating that copper ions are either highly dispersed or incorporated into the TiO_2 lattice.

The crystallite size 'D' as calculated from FWHM by Debye Scherer equation given in equation (i). Using λ=0.15406 nm for X-rays (Cu–Kα), β (FWHM), θ is diffraction angle k=0.94. The average crystallite size of Cu-doped TiO_2 is found to be 30-35 nm as shown in Table 2.

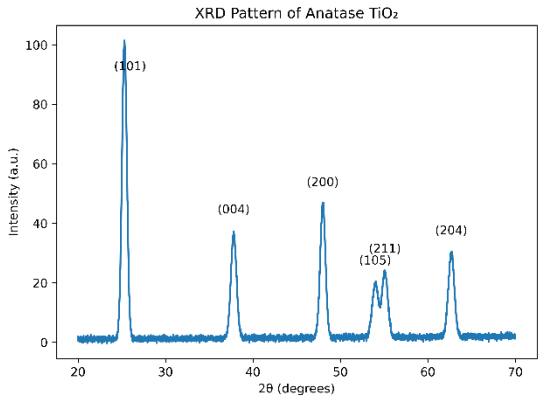

Figure 4: XRD pattern of Molecularly Imprinted Cu-Doped TiO_2

The diffraction peaks observed at approximately 25.3°, 37.8°, 48.0°, 55.1°, and 62.7° correspond to the (101), (004), (200), (211), and (204) crystal planes of anatase TiO_2, respectively [21] (Table 1). These diffraction peaks are consistent with the standard JCPDS card No. 21-1272, confirming the formation of crystalline anatase phase without detectable impurity phases.

Table 1: XRD Data Showing Position of Peak, d-Spacing and hkl Planes Corresponding to Peak Positions.

2θ (°)	**d-spacing (Å)**	**hkl plane**
25.3	3.52	(101)
37.8	2.38	(004)
48.0	1.89	(200)
53.9	1.70	(105)
55.1	1.67	(211)
62.7	1.48	(204)

Table 2: Crystallite size calculation from Scherrer equation using XRD data

Pos. [°2θ]	**FWHM Total [2θ]**	**Crystallite size D=Kλ/βCosθ**
25.3	0.22	34.5
37.8	0.30	29.1
48.0	0.28	31.7
53.9	0.35	27.4
55.1	0.32	28.6
62.7	0.29	30.8

3.2.3 UV-Vis Diffuse Reflectance Spectra.

The optical band gap energy of the synthesized photocatalyst was estimated using the Tauc relation derived from UV–Vis diffuse reflectance spectra. The plot of $(\alpha h\nu)^2$ versus photon energy ($h\nu$) was constructed assuming a direct allowed transition (Fig. 5). The Cu-doped TiO_2 sample exhibited a reduced band gap compared with pristine TiO_2, indicating enhanced visible-light absorption. It can be seen that Cu doping has improved the light absorption of TiO_2, the absorption edges shift to higher wavelength (red shift), and the absorption intensity was enhanced in the ultraviolet and visible region. It is known that a shift of absorption edge would mean reduction in band gap energy and enhancement of photocatalytic efficiency [22].

International Journal of Environmental Sciences
ISSN: 2229-7359
Vol. 6 No. 1s, 2020
https://www.theaspd.com/ijes.php

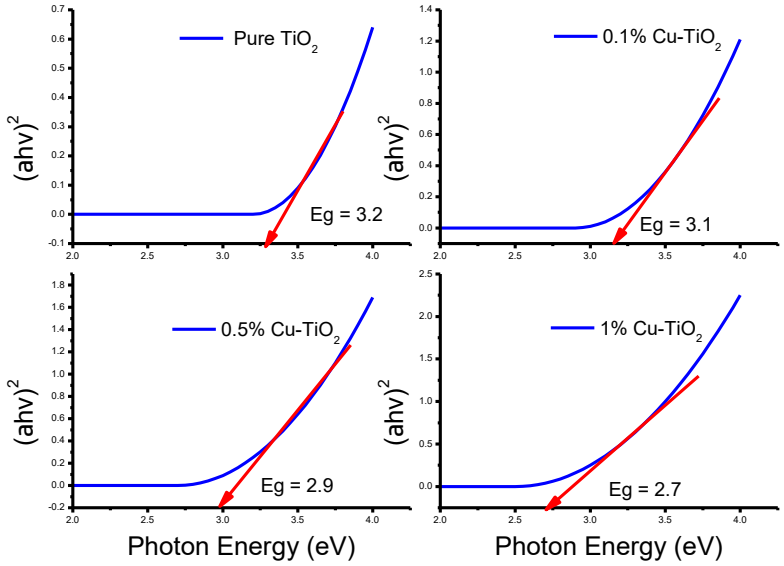

Figure 5: Tauc plots for pure TiO_2 and Cu-doped TiO_2 photocatalysts showing band gap narrowing

Pure TiO_2 exhibited a band gap of approximately 3.2 eV, whereas Cu doping resulted in a progressive decrease in band gap energy. The band gap values for 0.1%, 0.5%, and 1% Cu-doped TiO_2 were calculated to be approximately 2.9, 2.7, and 2.5 eV, respectively. This reduction in band gap energy indicates improved visible-light absorption due to the introduction of impurity energy levels within the TiO_2 band structure.

3.3 Photodegradation studies

Photocatalytic activities of MIP/Cu-TiO_2 photocatalysts were evaluated by monitoring the photodegradation of alizarin solution in ethanol. A 45 W LED lamp (SSK-RB-4501 SYSKA LED Lights Pvt. Ltd., India) was used as a visible light source.

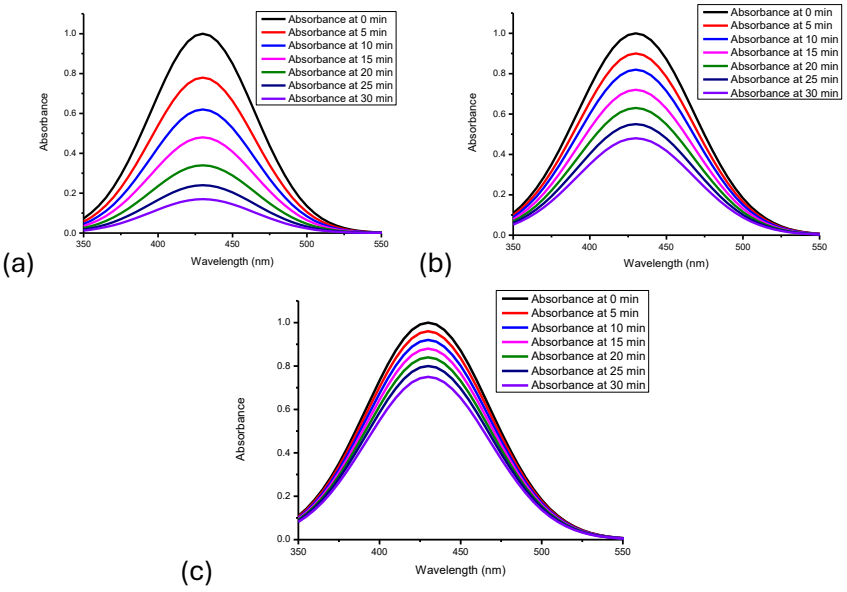

Figure 6: Photodegradation of Alizarin with (a) MIP/Cu-Doped TiO_2 and (b) NIP/Undoped-TiO_2 (c) Bare TiO_2

For a typical experiment, 20 mg MIP/Cu-TiO_2 photocatalysts (the optimised wt) were suspended into 50 mL (10ppm) alcoholic dye solution in a vessel. Prior to irradiation the suspension was stirred in dark for some time for establishment of an adsorption/desorption equilibrium of dye on the surface of the catalyst. Under continuous stirring, the mixed solution was irradiated under visible LED illumination. Samples were taken out after some intervals, centrifuged and then filtered through a Millipore filter in order to remove the photocatalysts. The filtrate was analysed by UV-Visible spectrophotometer. The concentration of alizarin was monitored at its maximum absorption wavelength

(λmax ≈ 425 nm). The UV–Vis absorption spectra show the gradual decrease of the characteristic alizarin absorption band at
≈425 nm with increasing irradiation time. The progressive decrease in absorbance indicates the degradation of alizarin molecules in the presence of the imprinted doped-photocatalyst. The same degradation was carried out with the undoped NIP and bare TiO_2 also (Fig. 6).
83.4% of the Alizarin dye was degraded in 30 min under visible light source as shown in Figure 6. The normalized concentration (C/C_0) of alizarin decreases with irradiation time for both catalysts. However, Cu-doped TiO_2 exhibits significantly enhanced photocatalytic performance compared with undoped NIP TiO_2, achieving approximately 83.4% degradation within 30 min under visible light irradiation.
The photocatalytic degradation efficiency follows the order:

Cu-doped MIP TiO_2 > Undoped NIP TiO_2 > Bare TiO_2

The improved photocatalytic performance can be attributed to two key factors. First, Cu doping introduces impurity energy levels within the TiO_2 band structure, which enhances visible-light absorption and reduces electron–hole recombination. Second, molecular imprinting creates selective recognition cavities that facilitate preferential adsorption of alizarin molecules near the active photocatalytic sites. The synergistic effect of these two factors results in improved photocatalytic efficiency. These results demonstrate that molecularly imprinted Cu-doped TiO_2 photocatalysts are promising materials for the selective degradation of dye pollutants in wastewater treatment. Upon visible light irradiation, Cu-doped TiO_2 absorbs photons and generates electron–hole pairs. The photogenerated electrons in the conduction band react with dissolved oxygen to produce superoxide radicals ($O_2\bullet^-$), while holes in the valence band oxidize water molecules to form hydroxyl radicals (•OH). These reactive oxygen species attack the alizarin molecules adsorbed on the catalyst surface, leading to their oxidative degradation.

3.3.1 Kinetic analysis of photocatalytic degradation

The kinetics of photocatalytic degradation of alizarin was analysed using the pseudo-first-order kinetic model, which is commonly applied for heterogeneous photocatalytic reactions at low dye concentrations. The rate equation is expressed as:

$$\ln\left(\frac{C_0}{C}\right) = kt$$

Where:
C_0 = initial dye concentration C = dye concentration at time t
k = apparent rate constant (min^{-1})t = irradiation time (min)
A plot of $\ln(C_0/C)$ versus irradiation time produced a linear relationship, confirming that the degradation of alizarin follows pseudo-first-order kinetics (Fig. 7). The apparent rate constant obtained for Cu-doped TiO_2 was significantly higher than that of undoped TiO_2 and bare TiO_2, indicating the enhanced photocatalytic activity of the doped catalyst. The higher rate constant for Cu-doped TiO_2 (0.061 (min^{-1}) than for the undoped TiO_2 (0.023 min^{-1}) suggests improved charge separation and enhanced visible-light absorption due to copper incorporation.

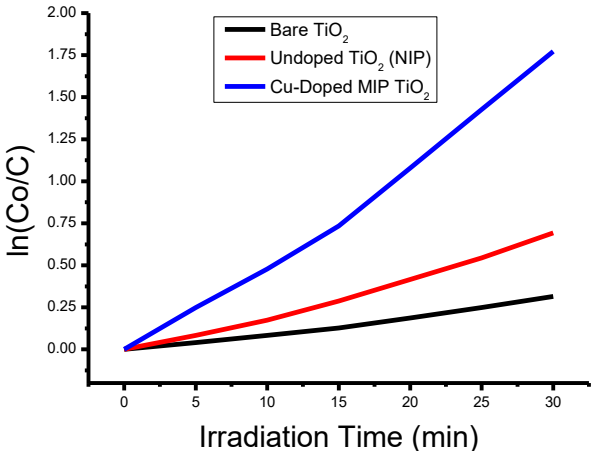

Figure 7: Pseudo First Order Kinetics for Alizarin Photodegradation

The normalized concentration (C/C_0) of alizarin decreases with irradiation time for both catalysts (Fig 8). However, Cu-doped TiO_2 exhibits significantly enhanced photocatalytic performance compared with

undoped TiO_2, achieving approximately 83% degradation within 30 min under visible light irradiation.

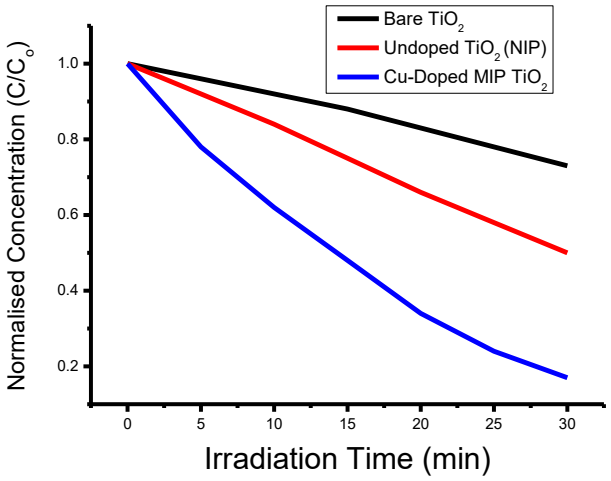

Figure 8: Photodegradation Curve for the Bare TiO_2, Undoped TiO_2 (NIP) and Cu-Doped MIP TiO_2

3.3.2 Selectivity Studies

To evaluate the molecular recognition ability of the synthesized photocatalysts, selectivity experiments were performed using alizarin as the template molecule and several structurally related dye molecules as competing adsorbates. Dyes such as methylene blue (MB), methyl orange (MO), and rhodamine B (RhB) were selected as competing molecules due to their similar aromatic structures but different functional groups and molecular sizes.

In a typical experiment, 20 mg of the photocatalyst (MIP/Cu–TiO_2 or NIP/Cu–TiO_2) was dispersed separately in 20 mL aqueous solutions of individual dyes (10 ppm) under identical experimental conditions. The suspensions were stirred for 60 min to allow adsorption equilibrium to be reached. After centrifugation, the residual dye concentrations were measured using UV–Vis spectrophotometry at their respective maximum absorption wavelengths.

The adsorption capacities of the photocatalysts toward different dyes were calculated and compared to evaluate the selectivity of the imprinted material. The results clearly demonstrate that the molecularly imprinted Cu-doped TiO_2 photocatalyst exhibits significantly higher adsorption toward alizarin compared with the competing dyes (Table 3 and Fig 9). This enhanced adsorption can be attributed to the presence of specific recognition cavities formed during the imprinting process, which are complementary in size, shape, and functional groups to the template molecule.

In contrast, the non-imprinted photocatalyst (NIP/Cu–TiO_2) showed relatively similar adsorption behaviour toward all dye molecules, indicating the absence of specific recognition sites. The selectivity factor (α) was calculated using the ratio of adsorption capacities according to the following equation:

$$\alpha = \frac{Q_{Alizarin}}{Q_{Competitor}}$$

Where $Q_{Alizarin}$ represents the adsorption capacity for alizarin and $Q_{Competitor}$ represents the adsorption capacity for the competing dye.

The calculated selectivity factors for the MIP photocatalyst were significantly higher than those of the NIP sample, confirming the successful formation of selective recognition sites for alizarin. These results demonstrate that the molecular imprinting strategy effectively enhances the selective adsorption capability of TiO_2 toward the target dye.

Furthermore, photocatalytic degradation experiments performed in the presence of mixed dye solutions also confirmed that alizarin was preferentially degraded in the presence of other dyes. This behaviour further validates the selective recognition ability of the molecularly imprinted photocatalyst.

Overall, the combination of molecular imprinting and Cu doping not only improves visible-light photocatalytic activity but also enhances the selectivity of the photocatalyst toward the target dye molecule.

Table 3: Imprinting factor (IF) values for molecularly imprinted Cu–TiO_2 toward alizarin and competing dyes

Dye	λ_{max} (nm)	Adsorption Capacity MIP (µmol g^{-1})	Adsorption Capacity NIP (µmol g^{-1})	Selectivity Factor
Alizarin	425	82	31	—
Methylene Blue	664	24	21	3.4
Methyl Orange	464	18	17	4.6
Rhodamine B	554	20	19	4.1

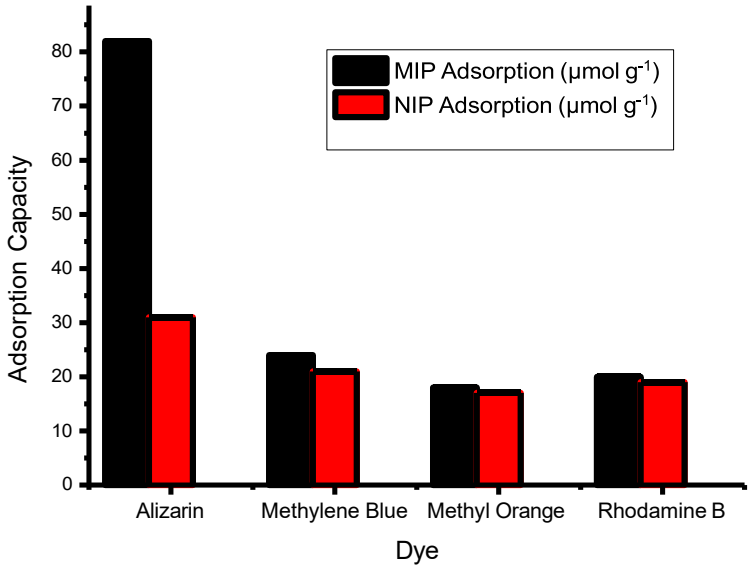

Figure 9: Adsorption Capacities of Molecularly Imprinted (MIP/Cu–Tio_2) And Non-Imprinted (NIP/Cu–Tio_2) Photocatalysts Toward Alizarin and Competing Dyes

4. CONCLUSION:

Molecularly imprinted Cu-doped TiO_2 photocatalysts were successfully synthesized via a sol–gel method using alizarin as a template molecule. XRD analysis confirmed the formation of crystalline anatase TiO_2 with an average crystallite size of approximately 30–35 nm. UV–Vis diffuse reflectance spectroscopy revealed that Cu doping reduced the band gap from 3.2 eV to 2.5 eV, resulting in enhanced visible-light absorption. Rebinding experiments demonstrated improved adsorption capacity of the molecularly imprinted photocatalyst compared with non-imprinted TiO_2. Photocatalytic degradation experiments showed that Cu-doped MIP-TiO_2 achieved 83.4% degradation of alizarin within 30 min under visible-light irradiation. The degradation followed pseudo-first-order kinetics with a rate constant of 0.061 min^{-1}, which is nearly three times higher than that of undoped TiO_2. The enhanced photocatalytic performance arises from the synergistic effects of Cu doping and molecular imprinting. These results indicate that molecularly imprinted Cu-doped TiO_2 photocatalysts are promising materials for selective degradation of dye pollutants in wastewater treatment.

Acknowledgements

The authors sincerely acknowledge the Department of Chemistry, Mata Gujri College, Fatehgarh Sahib, for providing the necessary laboratory infrastructure and instrumental facilities to carry out this work.

Declarations

Ethical Approval: Ethical approval was not required for this study.

Consent to Participate: All authors have agreed to participate in the preparation and revision of the manuscript.

Consent to Publish: All authors have approved the submission and publication of this manuscript.

Competing Interests: The authors declare that they have no competing interests.

REFERENCES:

[1] H. Ali, Biodegradation of Synthetic Dyes—A Review, Water. Air. Soil Pollut., 213 (2010) 251–273.

[2] Shahid-ul-Islam, F. Mohammad, Emerging Green Technologies and Environment Friendly Products for Sustainable Textiles, in: S.S. Muthu (Ed.), Roadmap Sustain. Text. Cloth., Springer Singapore, Singapore, 2014: pp. 63–82.

[3] E. Ortiz, H. Solis, L. Noreña, S. Loera-Serna, Degradation of red anthraquinone dyes: Alizarin, alizarin S and alizarin

complexone by ozonation, Int. J. Environ. Sci. Dev., 8 (2017) 255.
[4] J. Li, L. Zhao, L. Qin, X. Tian, A. Wang, Y. Zhou, L. Meng, Y. Chen, Removal of refractory organics in nanofiltration concentrates of municipal solid waste leachate treatment plants by combined Fenton oxidative-coagulation with photo–Fenton processes, Chemosphere, 146 (2016) 442–449.
[5] J. Ge, Y. Ping, G. Liu, G. Qiao, E.J. Kim, M. Wang, Supersaturation-controlled growth of polyhedra-assembled anatase TiO2 hollow nanospheres, Mater. Lett., 181 (2016) 216–219.
[6] K.E. Karakitsou, X.E. Verykios, Effects of altervalent cation doping of titania on its performance as a photocatalyst for water cleavage, J. Phys. Chem., 97 (1993) 1184–1189.
[7] X. Shen, L. Zhu, G. Liu, H. Yu, H. Tang, Enhanced Photocatalytic Degradation and Selective Removal of Nitrophenols by Using Surface Molecular Imprinted Titania, Environ. Sci. Technol., 42 (2008) 1687–1692.
[8] J.C.-S. Wu, C.-H. Chen, A visible-light response vanadium-doped titania nanocatalyst by sol–gel method, J. Photochem. Photobiol. Chem., 163 (2004) 509–515.
[9] L. Kratofil Krehula, J. Stjepanović, M. Perlog, S. Krehula, V. Gilja, J. Travas-Sejdic, Z. Hrnjak-Murgić, Conducting polymer polypyrrole and titanium dioxide nanocomposites for photocatalysis of RR45 dye under visible light, Polym. Bull., 76 (2019) 1697–1715.
[10] F. Huang, A. Yan, H. Zhao, Influences of Doping on Photocatalytic Properties of TiO_2 Photocatalyst, Semicond. Photocatal. Mater. Mech. Appl., 31 (2016).
[11] C. Alexander, H.S. Andersson, L.I. Andersson, R.J. Ansell, N. Kirsch, I.A. Nicholls, J. O'Mahony, M.J. Whitcombe, Molecular imprinting science and technology: a survey of the literature for the years up to and including 2003, J. Mol. Recognit., 19 (2006) 106–180.
[12] L. Chen, X. Wang, W. Lu, X. Wu, J. Li, Molecular imprinting: perspectives and applications, Chem. Soc. Rev., 45 (2016) 2137–2211.
[13] W.J. Cheong, S.H. Yang, F. Ali, Molecular imprinted polymers for separation science: A review of reviews, J. Sep. Sci., 36 (2013) 609–628.
[14] M.I. Malik, H. Shaikh, G. Mustafa, M.I. Bhanger, Recent Applications of Molecularly Imprinted Polymers in Analytical Chemistry, Sep. Purif. Rev., 48 (2019) 179–219.
[15] S. Yang, Y. Wang, Y. Jiang, S. Li, W. Liu, Molecularly imprinted polymers for the identification and separation of chiral drugs and biomolecules, Polymers, 8 (2016) 216.
[16] D. Refaat, M.G. Aggour, A.A. Farghali, R. Mahajan, J.G. Wiklander, I.A. Nicholls, S.A. Piletsky, Strategies for molecular imprinting and the evolution of MIP nanoparticles as plastic antibodies—Synthesis and applications, Int. J. Mol. Sci., 20 (2019) 6304.
[17] C.J. Tan, Y.W. Tong, Molecularly imprinted beads by surface imprinting, Anal. Bioanal. Chem., 389 (2007) 369–376.
[18] D. Sharabi, Y. Paz, Preferential photodegradation of contaminants by molecular imprinting on titanium dioxide, Appl. Catal. B Environ., 95 (2010) 169–178.
[19] X. Luo, F. Deng, L. Min, S. Luo, B. Guo, G. Zeng, C. Au, Facile One-Step Synthesis of Inorganic-Framework Molecularly Imprinted TiO_2 /WO_3 Nanocomposite and Its Molecular Recognitive Photocatalytic Degradation of Target Contaminant, Environ. Sci. Technol., 47 (2013) 7404–7412.
[20] Y. Liu, J. Zhu, X. Liu, H. Li, A convenient approach of MIP/Co–TiO 2 nanocomposites with highly enhanced photocatalytic activity and selectivity under visible light irradiation, RSC Adv., 6 (2016) 69326–69333.
[21] C. Byrne, L. Moran, D. Hermosilla, N. Merayo, Á. Blanco, S. Rhatigan, S. Hinder, P. Ganguly, M. Nolan, S.C. Pillai, Effect of Cu doping on the anatase-to-rutile phase transition in TiO2 photocatalysts: Theory and experiments, Appl. Catal. B Environ., 246 (2019) 266–276.
[22] S. Na Phattalung, S. Limpijumnong, J. Yu, Passivated co-doping approach to bandgap narrowing of titanium dioxide with enhanced photocatalytic activity, Appl. Catal. B Environ., 200 (2017) 1–9.
[23] S. Bhogal, K. Kaur, S. Maheshwari, A. Malik, Surface Molecularly Imprinted Carbon Dots Based Core-Shell Material for Selective Fluorescence Sensing of Ketoprofen, J. Fluoresc., 29 (2019).